JOURNAL OF MECHANICS OF CONTINUA AND MATHEMATICAL SCIENCES
www.journalimcms.org

ISSN (Online) : 2454 -7190 Vol.-17, No.-1, January (2022) pp 104-116 ISSN (Print) 0973-8975

AN EFFICIENT NUMERICAL SCHEME FOR STATIC TORQUE PROFILING OF SWITCHED RELUCTANCE MACHINE WITH EXPERIMENTAL VALIDATION

Sanam Rehman Mahar[1], Muhammad Mujtaba Shaikh[2]
Ali Asghar Memon[3]

[1]IICT, Mehran University of Engineering and Technology, Jamshoro, Pakistan.

[2]Department of Basic Sciences and Related Studies, Mehran University of Engineering and Technology, Jamshoro, Pakistan.

[3]Department of Electrical Engineering, Mehran University of Engineering and Technology, Jamshoro, Pakistan.

Corresponding Author: **Muhammad Mujtaba Shaikh**

Email: mujtaba.shaikh@faculty.muet.edu.pk

https://doi.org/10.26782/jmcms.2022.01.00008

(Received: November 11, 2021; Accepted: December 27, 2021)

Abstract

In AC and DC drives, the use of switched reluctance machine (SRM) is becoming popular as it has a few preferences over AC and DC drives in a simple and robust construction without brushes, low inertia, and high torque to weight ratio, without rotor windings, simple circuit power converter, etc. SRM is widely used in variable speed and servo drives. Because of the double saliency structure and the high nonlinearity of magnetic material, it is difficult to represent the flux-linkage and static torque characteristic of the SRM. This work promotes the use of an improved numerical integration scheme for the static characteristics of SRM. The static torque function that depends on the rotor position and the phase current of the flux linkage features family (for different rotor positions) is improved in the proposed work. Firstly, we use an experimental setup for the electromagnetic characteristic of SRM. Then, we use the improved scheme to develop an efficient mathematical model for static characteristics and finally simulate the static characteristic of SRM through MATLAB code. In the last step, we compare the performance of the proposed integrator model with an existing approach for better efficiency of the static characteristic of SRM with experimental validation.

Keywords: Numerical scheme, Switched Reluctance machine, Static Torque, Numerical Integration. Experimental Validation.

I. Introduction

The initial idea of SRMs was taken in 1814. In the last few decades, these motors were reinvented and put to practical use in line with the advancement of electronic power equipment. The switched reluctance machine (SRM) is becoming popular as it has a few preferences over AC and DC drives. because it has simple and

robust construction without brushes, high efficiency, high torque to inertia, high torque to weight ratio, and no conductor and permanent magnet on so it should be rotor-economic [XVII].

SRMs have salient poles in both the rotor and the stator and operate as a single-excited configuration with inactive (coil-free) rotors. The stator has a centralized winding system with multiple phases. The coils are fed from a DC power supply periodically and sequentially and thus create electromagnetic torque. SRMs have been of significant interest in the last two decades due to their simplicity and structural strength and are expected to find wider price and efficiency applications compared to other motors. Furthermore, several experiments have been carried out to boost the efficiency of these motors as a possible alternative to AC (asynchronous and synchronous) motors. Switched reluctance motors are currently in their infancy in commercial terms, but they are predicted to be used more commonly used shortly.

The cross-section of a typical four-phase (8/6) SRM is shown in Fig. 1, where for the sake of lucidity a single phase coil was drawn together with a power converter. On both the stator and rotor, the SR motor is salient, singularly excited (stator only), and brushless. The rotor, made from a stack of laminated steel, does not have magnets or windings. On its poles, the stator houses concentrated windings, and diametrically opposite stator pole windings are linked in series to form one phase. (as shown in Fig.1). Implicitly, the conversion of electromechanical energy can be regarded as the successful conversion of electrical energy into magnetic energy and of magnetic energy into mechanical energy usually linked by differential equations [XV].

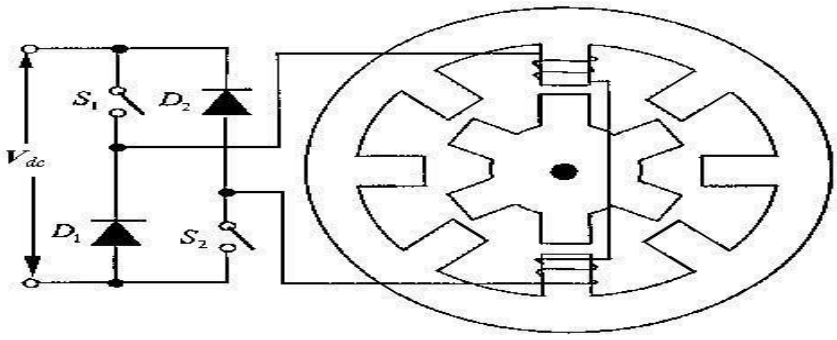

Figure 1. The cross-section of a typical four-phase (8/6) SRM

In literature, many academic studies have been performed in the past few decades: A variety of methods have been suggested as

1. Modeling of magnetic features by means of computer programming.
2. Analyzing the linkage of flux directly through magnetic sensor within the motor.
3. Inductance measurement directly.
4. Indirectly measuring the linkage of flux.

Studies on the SRM study have stated that most of the papers recommend explicitly using a magnetic sensor to test the flux linkage within the motor. This mechanism is not commonly introduced, since it is very expensive. When the motor is mounted, it

needs sensors to be built, thereby complicating the motor design. The flux sensor may not be able to accurately quantify a large range of flux variations. The static attributes, such as static torque, are based on finite element method (FEM) analysis. However, due to the choice of the elements used, the precision of these approaches varies, and they are dynamic in terms of computation. Secondary impacts such as manufacturing irregularities, three-dimensional (3-D) fields, and non-uniform iron structure, are difficult to model [V]. For different values of currents, the procedure for finding the motor characteristics is to calculate the motor inductance using the direct method. AC bridge techniques can assess motor inductance. These are essentially restricted to low-power machines as additional devices are required to an AC signal is overlaid on a broad DC that is introduced into the motor phase. Some studies have been proposed for the quantitative analysis of the SRM's complex features. Therefore, the optimal configuration of the SRM has not been thoroughly explained. For estimating the flux linkage characteristic, a personal computer or an oscilloscope have been used in several recent techniques. A drawback of these methodologies, however, is that the calculation is not fully automated when it comes to controlling motor voltage switching during the test or providing sensor calibration. Another setback of this approach is that several measurements must be carried out at each angle, making the procedure long. Other strategies are such as the search coil method [IV] and an integrator circuit [VI]. Another way to get these features by computer programming is the simulation process. An ANSYS package for 2-D transient analysis of the electromagnetic simulation model based on FE analysis was also used in [VIII]. Meanwhile, the authors also discussed the characteristics of the conventional SR motors with new topologies, referred to as segmental translator linear SR motors. The consequent properties of conventional and new SR motors were analyzed. In [III] authors used a stator flux estimation-based method and achieved improved estimations to stator flux and angles were achieved for SR machines by using some sensorless controllers. The actual voltage is maintained even at low-speed regimes, and the results were compared with experimental ones for various load and low-speed operations of the machine. Talani et al. in 2014 used cubic data interpolation and linear data interpolation techniques for determining static torque characteristics of SRM furthermore compared the results of both techniques to obtain the best curve fit [XXIII]. Ahmad and Narayanan (2016) used a mathematical model for calculating flux linkage feature with fewer parameters for all values of current and rotor ‘position by applying partial derivative and compared the results with Torey model, and reduced RMS error and calculating the back EMF for advanced controller [II]. Memon, Talani, and Memon (2016) experimental data table of flux linkage and inverted flux linkage are used to calculate co-energy, static torque respectively. The static characteristics of SRM are obtained using various data interpolation techniques and the results are finally compared for better performance [X]. Memon and Shaikh (2017) worked on the experimental method for determining the flux linkage for various values of (position and current) using search coil techniques. Moreover, static torque characteristic was obtained by locked rotor test simulation on LABVIEW (Laboratory Virtual Instrumentation Engineering Workbench) software [XII]. Memon et al. (2018) worked on the mathematical modeling of SRM and then compared two mathematical models, using different coding environments. The produced results were compared and validated with those obtained from the experiments, under the same operating

conditions for different performances of a switched reluctance machine. The simulation was done on MATLAB/SIMULINK software environment [XIII]. Uma, Kamalakannan, and Karthikeyan (2013) worked on the static and dynamic features of 8/6, 400W SRM using FEA software (MagNet 6.22) to obtain the torque and flux linkage characteristics, From the obtained flux linkage and torque characteristics to develop the torque and inductance profile and mathematical model on MATLAB/SIMULINK software [XXIV]. Shehata et al. (2018) presented a hardware-based experimental method for estimating the magnetic characteristic of SRM. Considering saturation and saliency, the machine phase characteristics (i.e. flux linkage, inductance) have a highly non-linear dependency on both phase current and position of the rotor. For calculating flux linkage and inductance characteristics using numerical integration technique, it is integrated by using Simpson's 1/3 rule [XXII]. Saha, Panda, and Panda (2018) discussed speed control and reduction in torque ripple by using the many optimizing liaison (MOL) methods and compared the results with those obtained by the Gravitational search algorithm (GSA) [XVI]. Memon et al. (2020) presented the static characteristics of the torque profile of the SRMs using numerical techniques. The experimental data tables of flux linkage and inverted flux linkage are used to compute co-energy using the numerical integrations method, which finally leads to computing the static torque profile of the machine using finite difference approximation. The computed torque profile obtained using numerical simulation in MATLAB software was compared with the measured torque profile obtained through experiments conducted on an existing 8/ 6-pole, 4-phase SR machine. To measure the accuracy of the computed torque profile and for its experimental validation, the statistical analysis of the results was carried out in terms of absolute and relative error (maximal positive, maximal negative, and mean) distributions in computed torque profile concerning the measured profile. The trend of both torque profiles is analyzed using a correlation study at different values of current. The accuracy of the computed torque profiles for an SR machine is demonstrated in terms of the statistical parameters. The comparison with experimental results was also carried out [XIV].

This work focuses upon the computation and improvement using numerical integration on four main data tables: flux linkage $\psi(\theta, i)$, inverted flux linkage, co-energy $W'(\theta, i)$ and static torque characteristics $T(\theta, i)$ for SRM. The static torque characteristics are the names given to these data tables. Out of the four tables of information, we use flux linkage data achieved from experiments, on an existing machine, using a software environment. Additionally, the static torque data from the experiments is extracted by using an existing machine from the locked rotor test. The improved integrator is suggested for co-energy making use of flux table. Finally, a finite difference approximation is used to approximate the static torque. The simulations are performed in MATLAB with the proposed model and an existing model. The results are validated based on error analysis and accuracy checks through experimental data.

II. Mathematical Model of Switched Reluctance Machines

To determine the phase current i, of the SRM, the basic simulation model used by many researchers including [XIV] is described by the following equations.

$$v = Ri + \frac{d}{dt}(\psi) \tag{1}$$

where v is the applied voltage, R is the winding resistance, and ψ is the flux linkage. Using a basic relationship between the flux linkage and current, i.e. (2) Equation (1) can be expressed as:

$$\psi = Li \tag{2}$$

Equation (1) can be expressed as

$$v = Ri + L\frac{di}{dt} + i\frac{dL}{dt} \tag{3}$$

If θ is the rotor position then, using chain rule in equation (3),

$$v = Ri + L\frac{di}{dt} + i\frac{dL}{d\theta}\omega \tag{4}$$

where $\omega = \frac{d\theta}{dt}$ is the angular speed rad/sec. where, the applied voltage is expressed as the sum of the resistive voltage drop, inductive voltage drop, and the induced EMF, respectively. To see the breakup of total power, vi, multiplying equation (4) by phase current i, leads to:

$$vi = Ri^2 + \frac{d}{dt}\frac{Li^2}{2} + i^2\frac{dL}{d\theta}\omega \tag{5}$$

Equation (5) shows that the total power is the sum of power loss, rate of increase of stored magnetic energy, and power converted from electrical energy to mechanical output power, respectively. The electromagnetic torque of SRM is given by equation (6)

$$T = i^2\frac{dL}{d\theta} \tag{6}$$

For dynamic characteristics of SRM, a mechanical equation (7) is added,

$$\frac{d\omega}{d\theta} = \frac{1}{J}(T - T_L) \tag{7}$$

where ω is used for rotational speed, T is used for the torque of the machine, T_L represents load torque, and J denotes the moment of inertia.

Once the data of induced EMF across the machine winding is available, the flux linkage ψ can be obtained using the relationship:

$$\int EMF\ dt = \psi \tag{8}$$

Having obtained flux linkage from (8), the relationship (2) can be used to calculate the inductance profile of the machine. The co-energy W' and the flux profiles of the SRM depending on current measurements i and the position θ are related by equation (9):

$$\mathrm{W}(\theta, \mathrm{i}) = \int_0^i \Psi(\theta, \mathrm{u})\mathrm{du} \tag{9}$$

Co-energy profile from equation (9) can be utilized for the computation of static torque $T(\theta, i)$ of the machine as described in equation (10)

$$T(\theta, i) = \frac{\partial \mathrm{W}(\theta,\mathrm{i})}{\partial \theta} \tag{10}$$

III. Experimental Data

Experimental data collection and measurement which forms the basis for further investigation in this work is taken for granted using the techniques is described in [I], [XII]. The data tables of induced EMF in the search coil of an existing switched reluctance prototype with the defined pole structure equipped with asymmetrical converter with 4-phase connections of SRM are explained in [I], [XII]. We require EMF data to calculate flux linkage by equation (8). It is obvious to mention that the inductance is maximum at the aligned position and minimum at the unaligned position, whereas the case of reluctance is reverse-natured at these positions. It is necessary to have a pattern of producing results that are comparable to the experimental to have accurate modeling and reliable machine performance. The flux table was collected using the Lab VIEW tool for an SRM with characteristics: D-80, 0.75 kW, and 1500 rpm. The obtained flux linkage characteristics for different positions and currents are shown in Figure 2 with a 3D view of flux linkage features concerning different rotor positions and currents.

The experimental data of static torque was acquired using a dynamometer employing a locked rotor test and allowing current to flow through the motor winding. The static torque data through experiments is summarized at some points in Table 1. The experimental torque profile is further explained in the results section and will be used for the validation of simulation results.

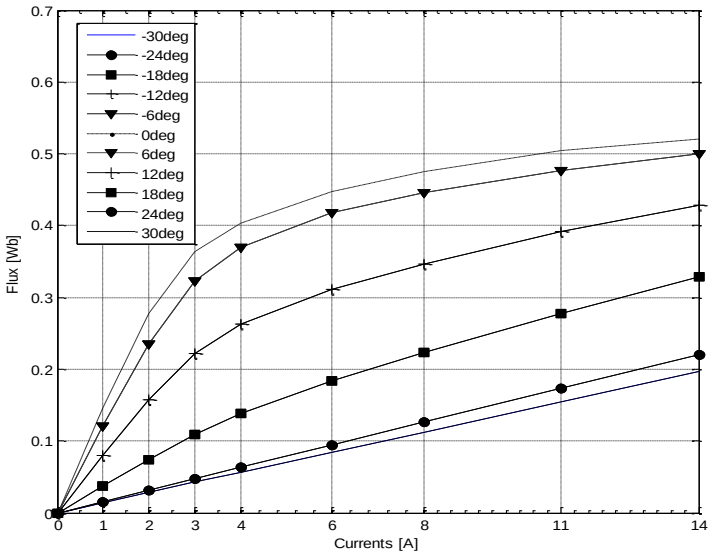

Figure 2. Measured flux linkage characteristics

Table 1: Measured static torque of the machine

Currents [A]	Position [deg.]	Measured static torque [Nm]
2	0	0
	-6	0.1762
	-12	0.1176
4	0	0
	-12	0.2417
	-18	0.1236
6	0	0
	-18	0.3218
	-24	0.1580
11	0	0
	-6	1.3823
	-24	0.4501

IV. Efficient Numerical Scheme for the Computation of Static Torque Profile

Using the data of flux linkages, the static torque can be computed using numerical integration on $\psi(\theta, i)$ followed by numerical differentiation of $W'(\theta, i)$. The process is described here in detail.

Suppose $(a = 0, 1, .., n)$ be the $(n + 1)$ currents, and $\psi(\theta_a, i_b)$ be the corresponding flux linkages across some fixed positions θ_b $(b = 1, 2, .., m)$, the co-energy profile from equation (9) can be obtained by numerical integration of $\psi(\theta, i)$ concerning the current i.

For this purpose, a closed Newton-Cotes quadrature approximation [XIX], [VII] with p nodes, $Q_{(p)}$ is usually used, and for a fixed a, it is defined as:

$$W'_{ES}[(\theta_a, i_b)] \approx Q_{(P)}[(\theta_a, i_b)] = \sum_{r=0}^{P-1} Crh^{r+1} S_{p,r} \quad (11)$$

For comparison purposes in this study, we refer to the scheme through (11), also well-known as the Trapezoidal rule, as an existing scheme (ES) for the integration in (9). The variants of ES were successfully used in [XVIII] for solving Fredholm integral equations of the second kind and in [XI] for evaluating Riemann-Stieltjes integrals numerically. The ES for the coenergy in terms of the flux linkage data can be obtained by setting $p = 2$ in equation (11).

We propose an enhancement of ES (11) as suggested and used in [IX], [XI] for numerical cubature, and Riemann-Stieltjes integral here for the numerical simulation of static torque profile. The coenergy by using the proposed scheme (PS) can be defined as [IX], [XI]:

$$W'_{PS}(\theta_a, i_b) = W'_{ES}[(\theta_a, i_b)] + \frac{i_b^3}{12} \Psi_{ii}\left(\theta_a, \frac{i_a + i_b}{2}\right) \quad (12)$$

Once the coenergy profiles are computed for all currents, equation (8) can then be used with numerical differentiation on the co-energy profiles to compute the numerical torque profiles. Using a finite difference approximation of the partial derivatives of

$W'(\theta, i)$ concerning the position at a fixed current i_b in (10), we obtain the computed static torque profiles as follows:

$$T_{(\theta_a, i_b)} = \frac{\partial[W'((\theta_a, i_b)]}{\partial\theta} \approx \frac{W'\left(\theta_{a+1, i_b}\right) - W'((\theta_a, i_b)}{\theta_{a+1-\theta_a}}, a = 1,2,3, \dots, m \quad (13)$$

To evaluate the performance of the PS and ES against the experimental data, we also use a statistical framework which is explained here. The error distributions are used between both profiles for sensitivity analysis of the numerically computed static torque profiles concerning experimentally obtained static torque data.

Let i_b be some specified current, $MT(\theta_a, i_b)$ and $CT(\theta_a, i_b)$ denote the measured and computed torque profiles comprising of m-nodes concerning the positions θ_b, $b = 1, 2, \dots m$, respectively, then the mean measured torque and the mean computed torque at some i_b can be obtained by using equations (14) and (15), respectively.

$$\mu_{MT}(i_b) = \frac{\sum_{a=1}^{a=m} MT(\theta_a, i_b)}{m} \quad b = 0,1,2, \dots, n \quad (14)$$

$$\mu_{CT}(i_b) = \frac{\sum_{a=1}^{a=m} CT(\theta_a, i_b)}{m} \quad b = 0,1,2,3, .., n \quad (15)$$

To see the discrepancy in the measured and computed static torque profiles, at some specified current i_b, the absolute error distributions across all positions θ_a can be computed using (16) [XX], [XXI]:

$$|\varepsilon_{ib}| = |MT(\theta_a, i_b) - CT(\theta_a, i_b)|, \quad (16)$$

for all , $a, b = 0,1,2, \dots, n$

V. Results and discussion

Using equations (11)-(12) by applying to existing and improved numerical integration schemes on the measured flux profile (Figure 2) at various values of constant current from 0A to 14A concerning various machine positions from -30 to 30 degrees, we simulated MATLAB software environment. The data based on flux profile, as in Figure 2, is used to integrate coenergy concerning currents for all positions from -30 to 30 degrees and at various constant current ranges from 0 to 14A, and the results are shown in Figure 3 (a) and 3 (b) using the PS and ES, respectively.

After computation of approximate coenergy profiles of SRM by ES and PS, we compute static torque profiles by these using equation (13) for the implementation of the finite difference formula of the approximate partial derivative of coenergy concerning position as shown. The numerically computed static torque profiles through PS and ES are displayed in Figure 4 along with the experimental torque profile in third place to observe the trend and pattern of the approximations. We observe that for the node corresponding to current equal to 8A and positions around -12^0 and 12^0, the ES torque deviates from the experimental torque sufficiently as compared to the PS. Through Figure 4, in general, it is immediate to] see that the

results of static torque characteristic by PS is more accurate and closely approaches to experimental ones.

In Figure 5, we compare mean measured and simulated (through ES and PS) static torques of the machine at various constant currents by using equations (14) and (15), respectively. It is apparent that the mean static torques obtained through the proposed model are closer to the experimental mean torques as compared to the existing model. The mean torque values do not, however, exhibit the considerable difference between the performance of ES and PS, and due to this reason, the absolute error distributions for constant currents across all rotor positions have been shown in Figure 6 between the computed (ES and PS) and experimental torques using equation (16). The oscillations in the absolute error distributions are more frequent and higher for the ES as compared to the PS with reference measured torques. The highest absolute error in both schemes corresponds to the node with 8A current and rotor positions of -12^0 and 12^0. In general, we can see that the PS sufficiently reduces the error and the highest error has been 0.013 Nm in the PS instead of a peak error of 0.032 Nm of the ES. Thus, the PS outer-performs for more accurate numerical simulation of the static torque profile of SRMs as compared to the ES and results in values closer to the experimental values.

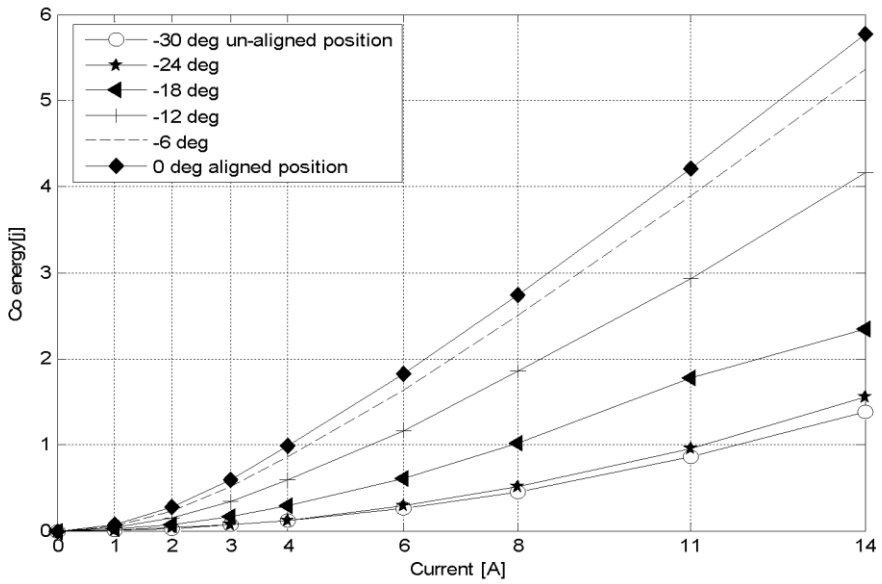

(a) Proposed scheme (PS)

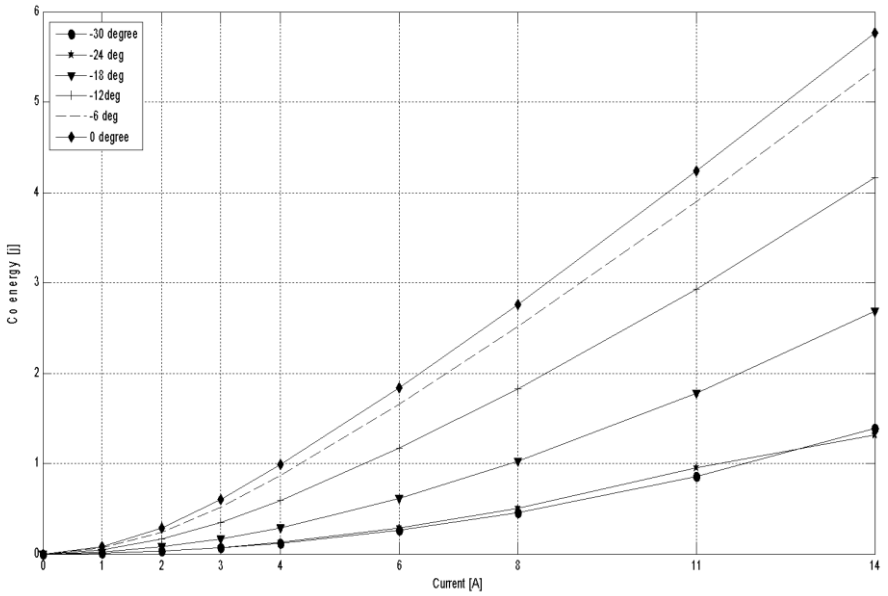

(b) Existing scheme (ES)

Figure 3. Numerically computed co-energy profiles vs current for different positions

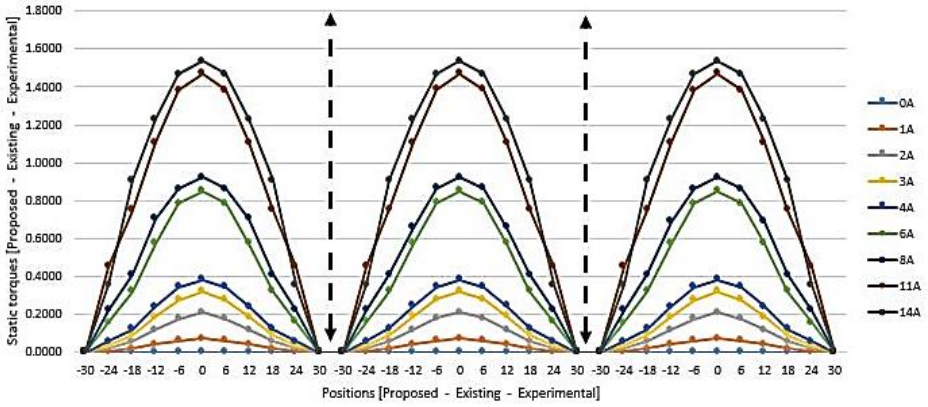

Figure 4. Static torque profiles (PS,ES,Experimental) at different positions and currents

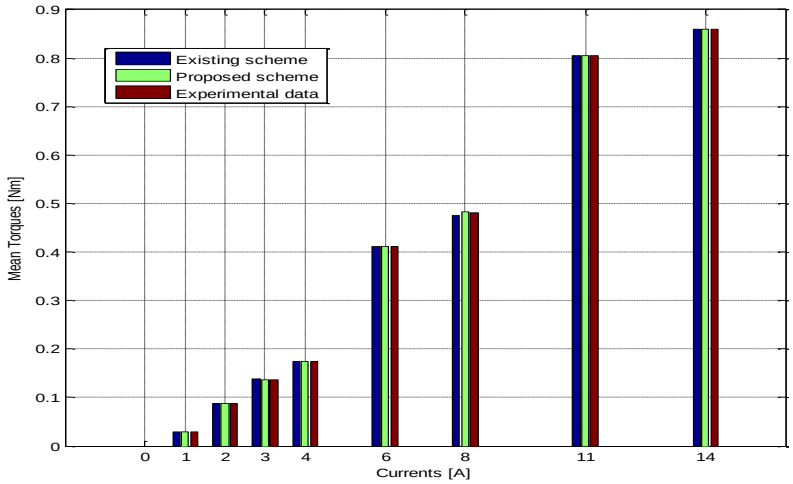

Figure 5. Mean computed (PS, ES) and measured torques at constant currents

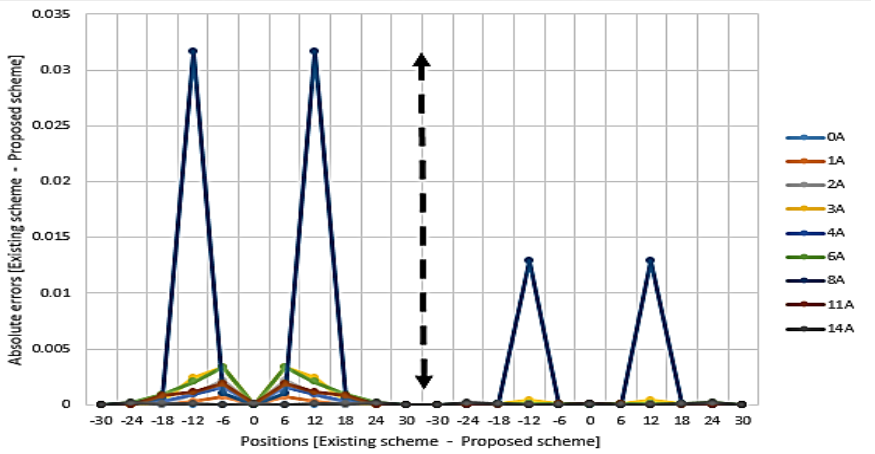

Figure 6. Absolute error distributions for ES and PS versus experimental static torque profiles at a different position for constant currents ranging from 0 to 14A.

VI. Conclusion

An efficient numerical scheme has been suggested for numerical simulation of static characteristics of SRMs with higher accuracy than an existing scheme based on experimental validation. The methodology was initiated with experimental input data of the flux linkage profile of the machine. Then, an advanced numerical integration approach was used to obtain coenergy table. Finally, the computed static torque characteristics were attained using a finite difference scheme. The results of static torque profiles of the proposed model were compared with the existing scheme with experimental torque as a reference of accuracy. Based on error distributions and comparison of torque profiles, it was observed that the proposed numerical scheme is more accurate with lesser errors and more efficient as compared to existing results. The comparison was based on the experimentally measured torque profiles of the machine. The proposed numerical scheme results have been validated successfully.

Conflicts of Interest:

The authors declare that they have no conflicts of interest regarding this article.

References

I. A. A. Memon (2012). Prediction of compound losses in a switched reluctance machine and inverter (Doctoral dissertation) University of Leeds (School of Electronic and Electrical Engineering), http://lib.leeds.ac.uk/record=b3231863.

II. Ahmad, S. S., & Narayanan, G. (2016). A simplified flux linkage characteristics model of switched reluctance machine. In 2016 IEEE International Conference Power Electronics, Drives and Energy Systems (PEDES) (pp. 1-6). IEEE.

III. Arias, A., Rain, X., & Hilairet, M. (2013). Enhancing the flux estimation. Electric power systems research, 104, 62-70.

IV. Charles V. Jones, "The Unified Theory of Electrical Machines", London, 1967.

V. Cheok, A. D., & Ertugrul, N. (2001). Computer-based automated test measurement system for determining magnetization characteristics of switched reluctance motors. IEEE Transactions on Instrumentation and Measurement, 50(3), 690-696.

VI. Corda J. (1979). PhD thesis, University of Leeds 1979.

VII. Dahlquist, G., & Björck, Å. (2008). Numerical methods in scientific computing, volume i. Society for Industrial and Applied Mathematics.

VIII. Ganji, B. and Askari, M.H., (2016). Analysis and modeling of different topologies for linear switched reluctance motor using finite element method. Alexandria Engineering Journal, 55(3), pp.2531-2538.

IX. Malik K., M. M. Shaikh, M. Saleem Chandio, A. W. Shaikh (2020). "Some New And Efficient Derivative-Based Schemes For Numerical Cubature", *J. Mech. Cont. & Math. Sci., Vol.-15, No.-10, Pp 67-78.*

X. Memon A. A., R. A. Talani, A. A. Memon (2016) Selecting best interpolation technique for simulation modelling of switched reluctance machine, Indian j.Sci Technol. 9 (16).

XI. Memon K., M. M. Shaikh, M. S. Chandio, A. W. Shaikh (2020). "A Modified Derivative-Based Scheme for the Riemann-Stieltjes Integral", Sindh Univ. Res. Jour. (Sci. Ser.) Vol. 52 (01) 37-40.

XII. Memon, A. A., and Shaikh, M. M. (2017). Input data for mathematical modeling and numerical simulation of switched reluctance machines. Data in brief, 14,138-142.

XIII. Memon, A. A., Shah, S. A. A., Shah, W., Baloch, M. H., Kaloi, G. S., & Mirjat, N. H. (2018). A flexible mathematical model for dissimilar operating modes of a switched reluctance machine. IEEE Access, 6: 9643-9649.

XIV. Memon, A. A., Shaikh, M. M., Bukhari, S. S. H., & Ro, J. S. (2020). Look- up data tables-based modeling of switched reluctance machine and experimental validation of the static torque with statistical analysis. Journal of Magnetics, 25(2), 233-244.

XV. Qing, Z. (2003). Modeling of switched reluctance motors for torque control.

XVI. Saha, N., Panda, A. K., & Panda, S. (2018). Speed control with torque ripple reduction of switched reluctance motor by many optimizing liaison technique. Journal of Electrical Systems and Information Technology, 5(3), 829-842.

XVII. Saxena, R., Singh, B., & Pahariya, Y. (2010). Measurement of Flux Linkage and Inductance Profile of SRM International Journal of Computer and Electrical Engineering, 2(2), 389.

XVIII. Shaikh, M. M., & Mujtaba, M. (2019). Analysis of polynomial collocation and uniformly spaced quadrature methods for second kind linear Fredholm integral equations – a comparison. Turkish Journal of Analysis and Number Theory, 7(4), 91-97.

XIX. Shaikh, M. M., Chandio, M. S., & Soomro, A. S. (2016). A modified four-point closed mid-point derivative based quadrature rule for numerical integration. *Sindh University Research Journal-SURJ (Science Series)*, *48*(2).

XX. Shaikh, M. M., Massan, S.-u-R. and Wagan, A. I. (2015). A new explicit approximation to Colebrook's friction factor in rough pipes under highly turbulent cases. International Journal of Heat and Mass Transfer, 88, 538-543.

XXI. Shaikh, M. M., Massan, S.-u-R. and Wagan, A. I. (2019). A sixteen decimal places' accurate Darcy friction factor database using non-linear Colebrook's equation with a million nodes: A way forward to the soft computing techniques. Data in brief, 27, 104733.

XXII. Shehata, A. M., El-Wakeel, A. S., Abdalla, Y. S., & Mostafa, R. M. (2018). Flux linkage and inductance measurement of a fault tolerant switched reluctance motor drive. In 2018 Twentieth International Middle East Power Systems Conference (MEPCON) (pp. 322-327). IEEE.

XXIII. Talani, R. A., Bhutto, G. M., Mangi, F. H., & Keerio, M. U. Comparative study of static torque characteristic of switched reluctance motor using spline and linear data interpolation techniques. Engineering, Science & Technology, 51.

XXIV. Uma, S., Kamalakannan, C., & Karthikeyan, R. (2013). Static and dynamic characteristics of 8/6, 400W switched reluctance motor. International Journal of Computer Applications, 66 (12), 1-8.